Fully Convolutional Architectures for Multi-Part Body Segmentation

J. Borrego Carazo
UB

August 13, 2018

Abstract

Contents

1 Introduction

Since the apparition of the powerful baseline system known as Fully Convolutional Network (FCN) several structures have been developed using the power of convolutions and avoiding the use of fully connected structures. For example, there are structures, such as [Rich features hierarchies*] or [Simultaneous Detection and Segmentation*], which are built for both tasks of detection and segmentation. Its main structure is defined by region proposal system, a further feature extraction structure based in CNN and a final classification method, such as SVM. Important to comment is the fact that some structures initially designed for detection such as Mask R-CNN [], use FCN modules to expand its capacity to do semantic segmentation, or in this case, instance segmentation. Also, among the structures that use CNN as its main core, stand out structures specific for semantic segmentation. They can be separated regarding they structural differences and, hence, different groups can be established: encoders-decoders which use pooling layers with skip connections [U-Net, Segnet] and those which use atrous or dilated convolutions [Dilated Convolutions, Deep Lab] among others. As a matter of fact, some of these structures add Conditional Random Fields (CRF) at the end of the network to refine the segmentation prediction, as in [DeepLab].

Nevertheless, it is also by the huge variety of applications of these networks and its outstanding performance that they have acquired great popularity. From the well known and established tasks of classification and object detection [YOLO, SSD], to the more recent tasks such as pose estimation [DeepPose] or action recognition [Action, 261advanced], and even text classification [advanced, 315]. Tasks which can be devoted to a wide range of data: biological [cancer], aerial [Aerial] and human [MPII pose] among others.

Our purpose is then to study the performance and behavior of fully convolutional networks regarding semantic segmentation but with a specific kind of data: human body parts. For this reason we have chosen the SURREAL data set. It provides around 6M frames from synthetically rendered 3D sequences of human motion data. As strong points stand out the variety and quantity of data, in terms of images but also of complementary information such as depth or body part joints, and also the easiness in its generation.

Considering our purpose, and having into account the limited time and space, several structures are going to be considered. To be able to have a differentiated analysis two different structures, regarding its segmentation procedure, has been selected: SegNet [] and Image Cascade Network (ICNet) []. Segnet is a encoder-decoder with skip connections that reuse the pooling indexes of the encoder in the decoder and ICNet is a cascade structure of different resolution branches which merge up to give a final segmentation. As commented, although both structures use CNN as its main component, both differ in the procedure or structure and then a differential study is presumed to be possible to be carried out.Nevertheless, only reference to general segmentation purposed networks has been defined. Among the networks which use CNN as its main component also stand out networks which are specific for certain types of objects. In our case, as we are studying the human body, we are interested in structures that can be specialized to obtain better results when dealing with images that contain such objects. Among these structures stand out those which use key points or pose information of the body to finally segment [Deep Multitask Architecture for Integrated 2D and 3D Human Sensing, Pose2Instance: Harnessing Keypoints for Person Instance Segmentation] it and also those which make use of the so called hourglass networks [SURREAL]. In our case we have selected stock hourglass. This decision is based on the supposed ease that the structure will allow for its study and change to observe the effects on the segmentation of the human body.

As stated, the work will have two main parts one devoted to general segmentation purposed structures and the other to human body specific structures. However, the procedure to implement them will be the same, that is: after having selected a recent article, an adequate code is searched either in Tensorflow or Keras. Once the code has been found suitable for the study several changes are applied to it. Mainly the code is prepared to accept our inputs and, if not are established, different metrics are included in the code.

Concluding the introduction, the purpose and definition of this work is to study the differences in performance and its reasosn of different deep neural networks which are mainly based on CNNs with respect to a specific dataset: SURREAL.

2 SURREAL Dataset

Deep neural structures stand out regarding accuracy results when large amounts of data are available for training. As manual annotation or supervision for obtaining ground truth data for tasks, such as ours, semantic segmentation, is expensive and time consuming, synthetic generation of this data has been used during the past years.

As real images are rich detailed in terms of textures, light, occlusions, shapes, the main problem regarding synthetic generation of data has been the reality of the images rendered. For this purpose, and as our task is semantic segmentation, we have chosen the SURREAL dataset (Synthetic hUmans foR REal tasks). The main reason is that it has a rich per-pixel ground-truth allowing the adequate training for tasks such as ours. As is stated in the original paper, the rendering is sufficiently realistic to allow knowledge transfer from the synthetic training images to testing real RGB images.

The resulting dataset consists of 6.5 million frames grouped into 67582 continuous image sequences of size 320x240. As the data is synthetically generated ground truths regarding optical flow, body part segmentation, depth, 3D and 2D joints and surface normals are also generated.

2.1 Image rendering procedure

The three main components of the data generation are: the creation of the synthetic body using the SMPL (a skinned multi-person linear model) body model, the fitting of its parameters by MoSH (Motion and shape capture from sparse markers), and the final rendering of the image from 3D sequences of motion capture (MoCap) data. The final results is a 3D human body with a random pose, random shape, random texture and rendered form a random point of view, random lightning and random background.

The main steps or components in the rendering or generating procedure are: body model, body shape, body pose, texture, light, camera, background and ground truth. The body model is initially defined using SMPL which decomposes body deformations into shape and pose. Shape is adjusted using a random sample from the CAESAR dataset and approximating it using SMPL shape components. Following, pose is fitted using as a reference a MoCap sequence and the 3D location of body markers that it has. The fitting is carried out by MoSh since transferring MoCap 3D data to a new model appears to be challenging. Next, two types of textures are used in the rendering process: the first one, which uses CAESAR scans and lacks of resolution and texture variety, and the second, extracted from 3D scans of subjects with normal clothing. All this rendering process for each image sequence is carried out with fixed light and camera conditions.

Regarding light the body is illuminated using Spherical Harmonics which coefficients are randomly sampled from a uniform distribution. In the case of the camera it is located for the viewpoint to point at the pelvis of the figure, positioned at a random distance and with random yaw angle. For the background, the person is rendered in top of a static image extracted from the LSUN dataset also to avoid having other human figures in the background. Finally, through different renderings of the image and the whole sequence through Blender all the ground truths are extracted and determined.

2.2 Dataset details and adaptation

The dataset is organized as the traditional package of training, validation and test data. The important unit of information is composed by 4 files: an *.mp4* image sequece (video), a segmentation, a depth and info files (in *Matlab* form, *.mat*). All these matrices include both ground truths and characteristics of the video sequence. Sequences are grouped regarding the characteristics of the pose and optical flow.

In each of the these categories (training, validation and test) there are 3 different partitions that reproduce the same sequences but with a main different characteristic: the overlap between one image sequence and the next is different. That is, in the first one we have a 30% overlap between consecutive sequences in the same group, and in the second a 50%, and a 70% in the third. Also, between them are differences regarding background, light, camera orientation and texture but not pose.

To obtain the final images and their ground truths we have followed a procedure and several modifications. First of all, in each of the segmentation files ground truth matrices for the segmentation of body parts. In each segmentation *mat* file are found as much matrices as frames have the corresponding video sequence. What has been done is to cut the video in the frames that is composed by and then all this frames have been saved as *jpg* images. Then each of the ground truth matrices in the segmentation file has been rendered as an image in the *png* format (this is very important since the *jpg* format for compressing an image changes the values of it and hence if the ground truth is saved in *jpg* the ground truth values are changed and its value broken). Then what is had is an RGB image and its associated segmentation ground truth with an integer value at each pixel ranging from 0 to 24 (the delimited body parts).

Secondly, after having all the images and ground truths in the adequate format we have selected a cluster of approx. 90k images for training from the 50% overlapping group, 15k for validation and 15k for testing. The clustering operation has been executed taking into account the 3D joints data of each of the bodies in the images.

Thirdly, to center the attention in the human body and taking into account that the background is static and plays no role further than background (no occlusions, nor human in the background) the images have been cropped. The procedure has been the following: the box that the body occupies is determined, the longer dimension of the box is selected, then an extra value is added to this dimension. This final length value is used for replacing the other shorter side of the box leaving a squared box which contains the human body inscribed in a reduced background with respect to the original image.

Finally, another operation on the image is needed to have the images ready used for training, validating and testing. The fact is that in the original ground truths there were some errors in the labels assigned to the chest and pelvis zones. In these zones there were pixels that had the head label assigned. Hence, the points had to be refilled with the appropriate values corresponding to each zone. The process used to achieve this was: select connected components with the label head, select all the areas except the bigger one (the head), using 8-connectivity refill the erroneous points with the maximum occurring value in their neighborhood.

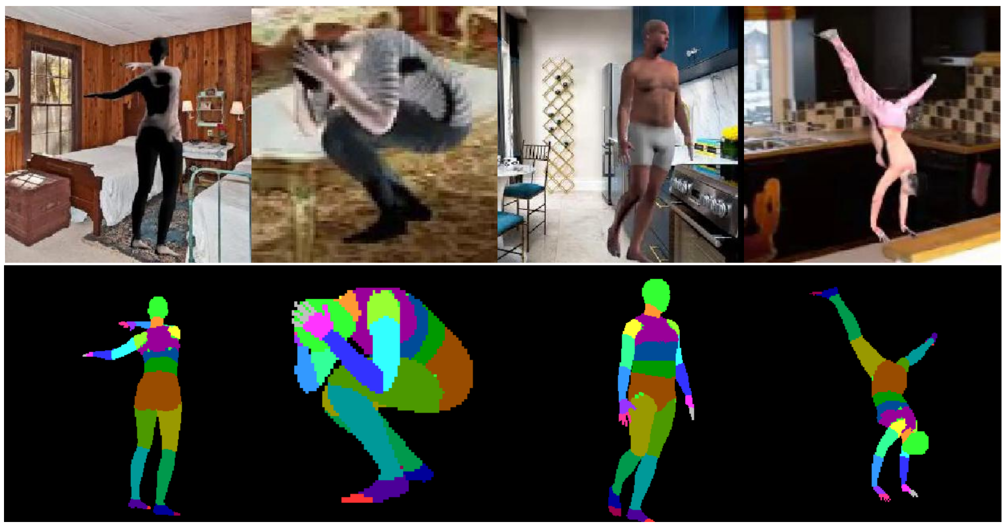

Figure 1: First row: sample images. Second row: corresponding ground truths

After all this procedure, the cluster images were prepared for training, validating and testing. In Fig 1 examples of the images and their respective ground truths can be observed.

3 General Segmentation Purposed Networks

3.1 Experimental Procedure

In this section the steps that will be followed when studying each network will be defined. The main purpose of doing so is to create a standardized procedure that helps in the reproduction of results, the study of the networks and the comparison between them. Regarding data, as it has not been specified yet, it suffices to state that we have training, validation and test sets.

First, with several, short, runs the hyper-parameters of the code, such as learning rate, batch size, among others, just to obtain the best combination and cope with other type of problems such as memory consumption. Once this has been done and the hyper parameters has been established the next step is to begin with ablation studies. However, and before that is important to check if some more modifications have to be made in the code, such as including validation performance recording, if it does not have it, just to make sure proper results will be obtained.

The ablation studies will consists on four modifications of the original network to see how it behaves. The modifications, that will be repeated for each network if possible, are:

- Doubling convolution filters
- Data augmentation: mirroring and scaling
- Class balancing through loss weighting

Before explaining each of the ablation procedures, it is convenient to explain the method that will be followed to apply them. First of all, the performance of the original network will be compared with the one with doubled filters. Then the best from the previous two regarding validation results will be compared to the network which includes data augmentation. Then, as before, the best from the previous comparison will be compared to the network with class balancing. Hence, the purpose of this ablation studies is, apart from seeing how the network behaves, to choose the best performing option. The training procedure is usually performed through 40k iterations (not epochs) on the training set, if another number is not specified. The performance result on the validation set is computed every certain number of steps, usually 200, to avoid runs that are too time consuming.

Finally, once the best performing network has been chosen it will be trained in a long run, always avoiding overfitting, and the network will be evaluated on the test set to obtain final results for this network. This results will, at the end, be useful to compare with the other networks studied.

The first ablation or modification is to double the quantity of filters of each convolution layer of the network. The main purpose of this change is related to the relationship between the variability of the data and the complexity of the network. If the original network is not sufficiently complex (does not has enough parameters) to absorb the diversity of the data an increase in filters may help the structure to get better results. However, if the original structure is already complex enough an increase in parameters will provoke, as usually, a reduction in the performance in the validation dataset due to the overfitting towards the training dataset. The purpose is the to study this possibilities.

Regarding the next ablation study, data augmentation, the purpose is related to the first ablation procedure. To add more diversity to the data and to end up with a more robust network against variability the data is augmented, mainly through mirroring and scaling. Mirroring in our case consists in a 180º degrees flip and scaling refers to the the image size modification.

Finally, the third change is adding a weighting to the loss. This is due to the fact that in the selected dataset there is a clear problem of unbalanced classes. Hence to compensate this, two strategies are devised to weight the loss regarding the weight of each class. As a multi class single label problem (as it is semantic segmentation) is faced the loss is computed through *softmax crossentropy*, hence having this loss in mind, the weighting methods consist in:

Direct strategy

$$L = -\sum_i y_i \log(softmax(x_i w_i))$$

where y_i is the label or ground truth, x_i is the output of the network and w_i is the vector of weights. The index i in this case refers to the class dimension in a one-hot encoding.

Outter strategy

$$L = -\sum_i w_i y_i \log(softmax(x_i))$$

In the first case, it can be seen that the weights are applied directly to the output values while in the second they are applied to the result of the crossentropy computation.

Nevertheless, there is one point left to state: how to choose the weights. Being C the total number of pixels in the training dataset, two methods have also been chosen in this case:

Inverse Frequency

$$W_i = 1 - \frac{C_i}{\sum_i C_i}$$

this weights will be marked as W1 throughout the work.

Exponential Weights

$$A = \frac{C}{max(C)}$$

$$B = \frac{1}{B}$$

$$W = Be^{-\frac{1}{4}\frac{B-mean(B)}{stdB}}$$

in this case *std* means standard deviation. This weights will be marked as W2 athrought the work.

**** REASON FOR THIS LAST WEIGHTS

Hence, what has been stated will be the main methodological procedure for this study. Nevertheless, the implementation of the specific steps is subject to the progress of the job. That is, and as will be seen, modification of the methodological procedure or further implementations will be applied as needed and at the light of the results obtained in the previous sections. This is done with the purpose of not establishing a specific and fixed methodology but rather a base for a further, deep and dynamic development of the study.

3.2 ICNet: Image Cascade Network

3.2.1 Introduction

Semantic segmentation methods based on CNN structures have improved largely the performance and have put offside methods based on hand crafted features. Among the CNN based methods there have been, mainly, two streams of development which have not been merged: high quality semantic segmentation methods and fast inference methods. In one hand, high quality methods, fueled initially by FCN (Fully Convolutional Networks), and further developed by works such as DeepLab or CRF (Conditional Random Fields), have centered their attention in obtaining as high as possible performance results. Thus, these methods have ended up without the possibility of being applied in real time scenarios. In the other hand, structures such as ENet or SegNet, have been created focused in high speed inference for semantic segmentation. Nevertheless and although these methods greatly raise the performance regarding efficiency, accuracy has been not maintained and has dropped to low levels. **bibliography

Hence, the main purpose of the design of the present network is to achieve fast semantic segmentation while maintaining decent prediction accuracy. Nevertheless, low resolution images would reduce inference and running time but would yield coarse, blurry outputs. In the contrary, high resolution inputs would be unbearable for the objective. Thus, To accomplish the objective low resolution images are used to high efficiency processing and to obtain a first but low quality segmentation feature map, while high quality is gained from high resolution images. Then, to merge both results a cascade framework is built in order to progressively refine segmentation predictions.

3.2.2 Description

The net is composed by three branches of different input resolutions and a cascade label guidance method (CCF: Cascade Feature Fusion Unit).

Low resolution. The input is downsampled to 1/4 of the original resolution and is passed through a FCN-based PSPNet architecture. The final output feature map, due to the pass through convolution layers, is 1/32 of the original resolution. After that the feature map is passed through several dilated convolution layers to enlarge the receptive field without downsampling the spatial size.

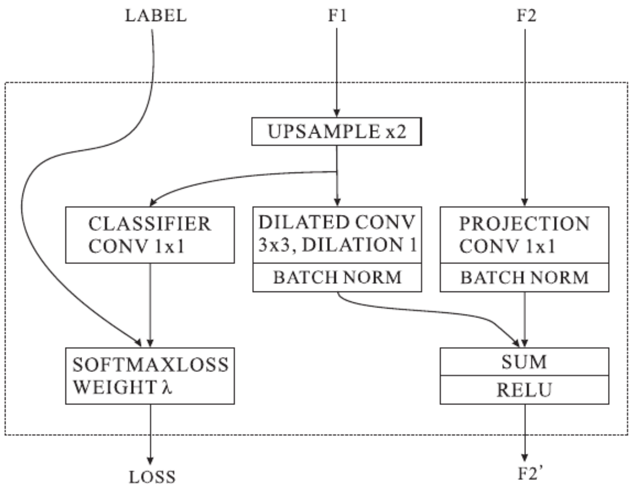

Figure 2: Cascade Feature Fusion unit. Two feature maps as inputs. One of the feature maps, coming from a lower resolution branch, has half of the resolution than the other input.

Middle resolution. The input is reduced to a 1/2 of the original resolution and after going through the convolution layers the outputted feature map has a resolution of 1/16 of the original image. Then through the Cascade Feature Fusion unit this output is merged with the output of the low resolution branch by upsampling the latter by a factor of 2.

High Resolution. As the middle resolution has already restored most semantic information the number of convolutions can be limited here. Three convolution layers are devised with kernel size 3x3 and stride 2 to go from an original resolution input to a 1/8 dowsample feature map. This feature map is combined through the CCF with the factor 2 upsampled map from the median resolution branch. Then the result is upsampled to resolution 1/4 and passed through a projection convolution.

CCF: Cascade Feature Fusion. As seen two feature maps are had. One, which comes each time from the lower resolution branch to the respective branch, has half the resolution. Then a dilated convolution with kernel size 3x3 and dilation 1 is applied to refine upsampled features. Following batch normalization layers are applied to each feature map and then a element wise SUM followed by a *ReLU* layer, ending up with both layers fused. This structure can be seen at Figure 2

Finally and regarding training, a softmax crossentropy loss is added to each branch producing three losses L_1, L_2 and L_3,

$$L = \lambda_1 L_1 + \lambda_2 L_2 + \lambda_3 L_3$$

where the λ_i are the weights applied to each branch loss. The network is then trained regarding the total loss. Has to be noted that, to gain efficiency at testing time the low resolution branches are not used and that the is expanded with one more upsampling to obtain an output of the resolution of the initial input. A global view of the architecture can be checked at Fig 3.

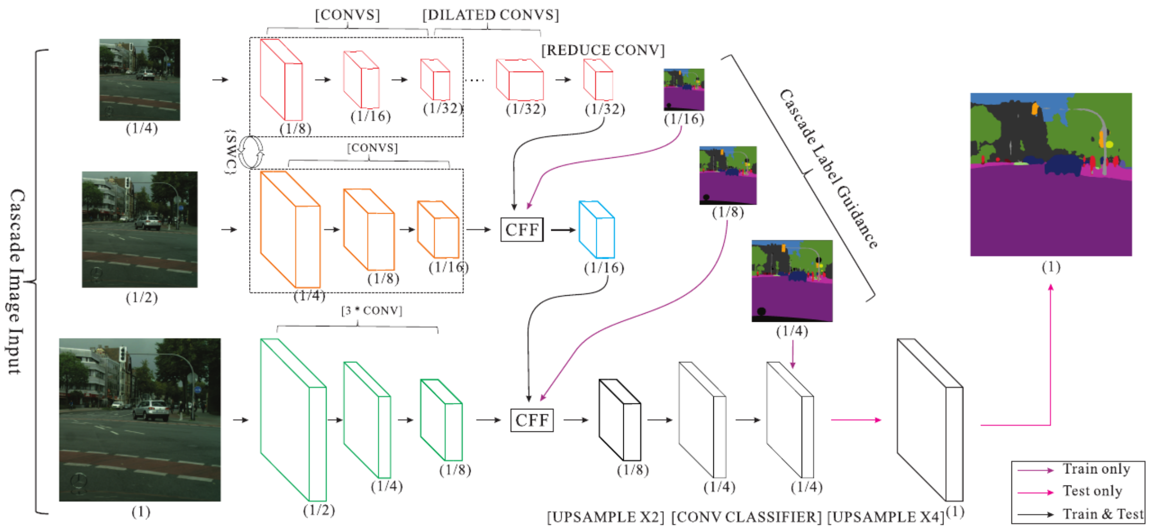

Figure 3: Sketch of the architecture of ICNet: the three resolution branches the CCFs and the points were the loss is computed. Also the specification of the use of each of the parts in terms of training and testing.

3.2.3 Results

The code used for this section can be found at hellochick/ICNet-Tensorflow.

Code adaptation. Several changes were made to the code in order to be able to apply it to our dataset and environment:

- Data input files.
- Input Size
- Number of classes and the ignored label.
- Enable loading of pretrained model by avoiding the load of final classification layers.
- Add validation structure
  - Created another instance of the class *Network*.
  - Establish the parameters as non trainable.
  - Copy the trained network into the validation network each time validation is carried out.
- Add metrics: F1, precision, recall, accuracy and accuracy per class.
- Add the possibility to weight loss according to each class importance.

After several finetunning purposed runs of the program the hyperparameters of the network has been set to the following values:

- Batch size 64
- Learning rate 0.01 and poly learning rate with power 0.9

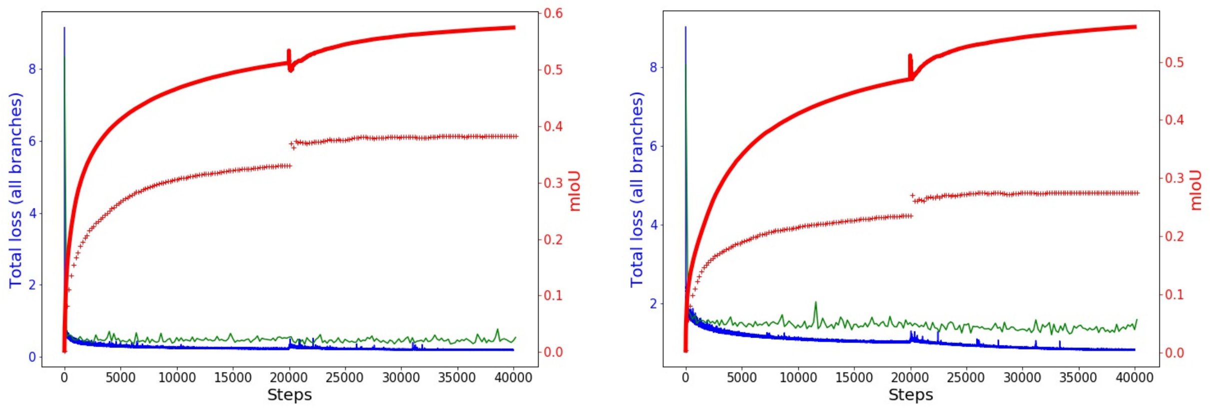

Figure 4: Loss plots for both normal (left) and with doubled filters (right) ICNet architectures. (Green) Validation loss, (Blue) Training Loss, training mIoU (red solid line) and validation mIoU (red crosses).

- Momentum 0.9 and weight decay 0.0001

The optimizer used corresponds to a momentum optimizer.

Ablation Results. To see which of the different possible configurations was the best performing one several runs have been carried out regarding number of filters, data augmentation and class balancing. The number of steps for training have been defined as 40000, the last 20000 with batch normalization parameter updating.

First of all, the performance on the validation set of normal structure and of the same one but with filters doubled are compared.

Architecture	**mIoU** (%)	**Accuracy** (%)	**F1** (%)
Normal	38.19	94.64	88.17
Doubled filters	27.51	93.01	84.97
Normal + Data Aug.	32.60	91.15	91.61

Table 1: Performance results on validation dataset for the normal structure and the architecture with doubled filters.

As seen in table 1, doubling the filters has not produced any gains. In Figure 4 the behavior of the losses as well as the metric mIoU in both training and validation datasets can be observed. It is seen that both developments are close to saturation, although in the doubled filters net there seems to be still space for training. Nevertheless, the evolution and results on the validation set are worse in this latter structure than in the normal one. Thus, and given this fact together with the saturation behavior, the normal net is preferred against the one with doubled filters.

Hence, and according to the methodology established in Section **??**, the results obtained next are the comparison between the best previous ablation, that is the structure without doubled filters, and the same net but with data augmentation. This is done with the intuition that the mirroring and scaling would help in making the net more robust during training and hence obtain a better result in the validation set. The results can be observed also in table 1. Has to be noted that, although the results regarding mIoU, and also accuracy, are worse compared to not using data augmentation, the performance regarding F1 is better. Nevertheless, as our metric of preference is mIoU we still have the normal structure as the best performing one.

Following, the normal structure is compared to the four different ways of applying class balancing to loss values (as established in **??**). Now the comparison is done through mIoU but also through accuracy per class to see the effects of the loss weighting. The results can be observed in table 2.

	mIoU (%)	**Accuracy per Class(%)**													
Architecture	**All Classes**	**All Classes**	**Background**	**Head**	**Torso**	**U.Legs**	**L.Legs**	**Neck**	**Shoulder**	**U.Arms**	**L.Arms**	**Feets**	**Hands**	**Fingers**	**Toes**
Normal	[38.2]	48.7	98.9	84.9	74.78	64.3	53.8	64.0	54.2	52.7	39.5	32.3	19.8	9.3	9.5
W1 (Outer)	37.5	52.3	97.7	90.0	74.8	70.9	61.7	60.9	56.0	57.34	50.1	38.9	22.9	10.2	11.3
W1 (Direct)	6.5	7.9	99.9	6.13	15.5	7.7	0.8	0.0	4.7	1.9	0.0	3.6	0.0	0.0	0.0
W2 (Outer)	25.8	[54.8]	89.2	89.3	61.6	64.1	65.2	72.4	60.3	47.0	46.03	52.35	33.4	31.0	36.9
W2 (Direct)	25.5	34.0	99.3	78.7	70.7	70.0	59.0	1.9	8.9	32.9	15.7	7.1	0.5	0.0	0 .0

Table 2: Performance results on validation dataset for the normal structure and the architecture with loss weighting for each setup. Here W1 indicates the inverse frequency weithing and W2 the exponential weighting.

Although the result of the loss weighting using the outer approach and the first set of weights has a performance similar to the normal structure, none of the results has surpassed the performance of the original structure. It can be observed, nonetheless, that the direct weighting is the worse in terms both of per class accuracy and mIoU. Although the first setup, among the weighting methods, has acquired the best mIoU result, the best balancing between classes in terms of accuracy has been achieved by the same method, that is outter balancing, but with the second set of weights.

Final Results. With the best setup regarding validation results, in this case the normal one with no additions, a training of 90k iterations is performed to achieve the best possible results.

Architecture	**mIoU (%)**	**Accuracy (%)**	**F1 (%)**
Normal	45.14	95.76	89.73

Table 3: Performance results on test set for the normal structure with a training of 90k.

In table 3 the results regarding mIoU, accuracy and F1 score for the normal structure in the test set and for 90k steps of training are presented. As it is obvious the performance is higher but not as much as expected taking into account that training steps more than doubled.

In Figure 5 qualitative results can be observed regarding the original structure with the 90k training.

3.2.4 Analysis and Conclusions

Regarding results shown in table 1, we can see that the normal net has got a better result in the validation set than the net with filters doubled. When the filters of a net are doubled, the parameters of the net, logically, get doubled. This can lead to two ends: the first, if

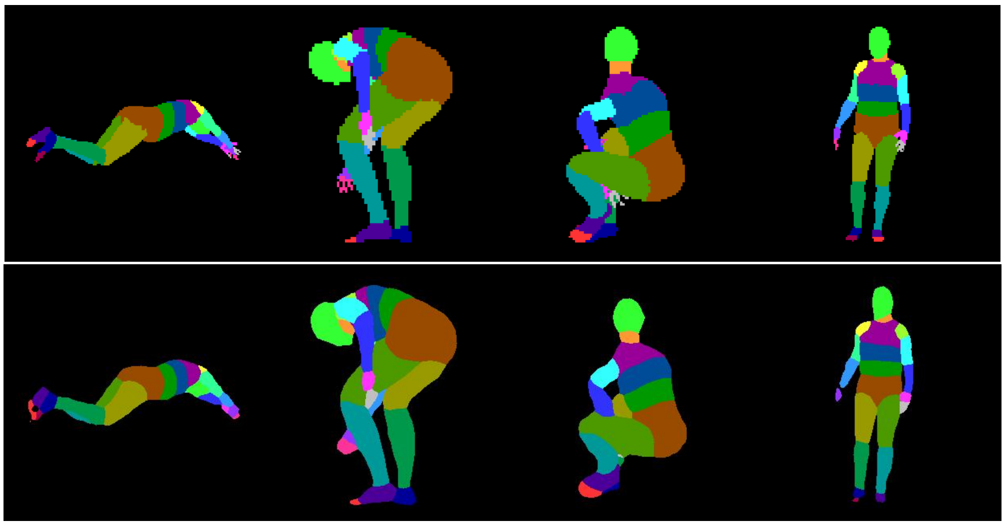
Figure 5: First row: ground truth examples. Second row: inference results with best ICNet model

the data is sufficiently complex to allow the net to train without overfitting, the results get better due to capturing more patterns or information, or, the second, that the excess filters make the whole net overfit to the training data since they capture elements only present in the training data but not in the validation. Hence, by the results shown, it is clear that what happened corresponds to the second case. This can also be seen in Figure 4 where the validation results are much worse almost at every step during the training for the doubled filters net. This clearly indicates, comparatively, an overfitting problem of the net.

Regarding the case of data augmentation, also in table 1, the problem may reside in that spatial information is important for learning the characteristics of the data. Hence, the distortions/modifications caused by the data augmentation, maybe disrupt the structure of this spatial informations. The main intention of data augmentation is make the net more robust to changes in the data, but maybe this effect is overcame by the disruption on the spatial data information.

In the case of the loss weighting scheme several statements can be made. First of all, the direct application of the weights has no use since it has not balanced the results at all. Next, regarding the outer application, although with the exponential weights the classes are more balanced in terms of accuracy (even the upper legs have obtained a better accuracy per class result than background), the result regarding mIoU is lower than in the original network. Comparing the results between the two outer method instances, one with the inverse frequency weights and the other with the exponential weights, one important thing can be commented: exponential weights seem to balance classes better while inverse frequency weights do not but obtain a better mIoU result. This can be due to the fact that trying to balance perfectly classes that account for a little area produces a poorer results if the main performance metric is related to area comparison.

** INCLUIR BatcH FIGURES ****

One important point to comment is the jump in the performance metric that appears in Figure 4. This jump corresponds to the inclusion of batch normalization variables into the trainable variables. Batch normalization consists in the following formulation

$$\beta + \frac{\gamma(x-\mu)}{\sigma} \tag{1}$$

In the first part of the training these variables, β,γ,μ and σ are not trained and correspond to fixed random values. When they are included into training its value gets adapted to the dataset. It is important then its inclusion. Nevertheless, the point at which they are included it is not significant since the behavior of the performance ens up being the same. Thus, it is only important that these inclusion into trainable variables takes place to obtain a proper training.

Regarding the final results on the test set, what can be established is that the structure is near saturation. That is training it more will not improve substantially the results. This can be deduced from Figure 4, where already was showing a little saturation, and from the fact that, with even more than doubling the steps, the results have not improved much. Also important to comment is the fact that, compared to the performance of the network used in the paper ***** on the Cityscapes dataset **** the result regarding mIoU is quite poor, since the authors obtain 67.7% mIoU on the test set. Nevertheless, in the case of the Cityscapes dataset the number of classes is 19.

On of the main reasons for this drop in performance could be that in our dataset a large (regarding pixel appearance frequency) and varied background which implies that the network spends part of its training learning to identify the background.

Nevertheless, if a look is taken at the qualitative results in Figure 5, it can be seen that they are quite acceptable. This statement is regarding body part definition and overall appreciation of the constituents of the body. The only body parts that lack of substantial definition are the extremities, such as fingers and toes which are bad defined or even not identified. Regarding variety of positions and occlusions of body parts it can be observed that the results are positive since the network has managed to learn the variety of body poses and occlusions regarding the body going out the frame.

As a conclusion, the results have been positive but not as high as expected. Also and surprisingly, all the ablation studies have resulted in no improvement of the performance results. In the case of the class balancing scheme, the direct method has proven to be a bad choice, hence it is discarded for further networks to be studied.

3.3 SegNet

3.3.1 Introduction

Regarding our task, which is semantic pixel-wise segmentation, most recent deep architectures share common or similar encoding parts, such as VGG-16 or ResNet. Even so, some of those approaches adapt structures oriented to one specific tasks, such as classification, to other tasks, such as semantic segmentation. This two facts have two big implications in the resulting networks. First, and commonly, the number of trainable parameters of the structure ascends to orders of hundreds of millions which makes difficult end-to-end training. This opens the way to multistage strategies such as task decoupling, appending heads to pre-trained base networks and other methods to ease the training process. Secondly, usually the output lacks of required definition, that is, appears coarse. This is mainly due to the reduction of resolution in the feature maps produced by max-pooling layers and other sub-sampling procedures. Solving these two hurdles will enable and efficient training and inference in terms of both memory and computation time.

Thus, the design and development of Segnet has been focused on both problems. This means having the requirement of a high quality mapping between low resolution features and input resolution pixel classification but without deepening or loading too much, just to avoid difficulties and inefficiencies at both inference and training time.

3.3.2 Description

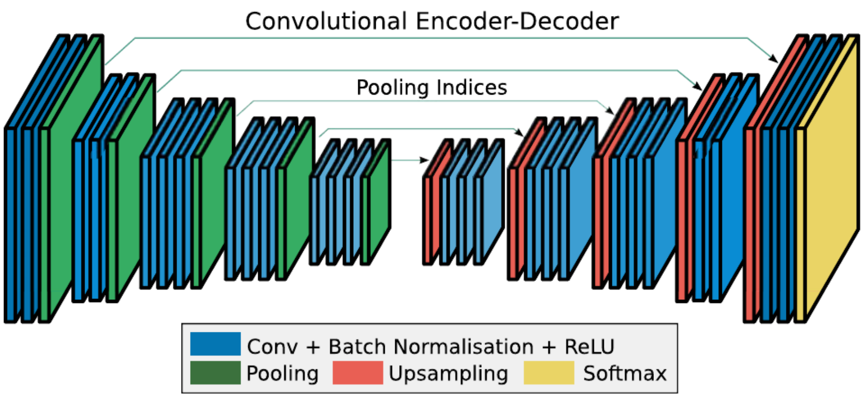
Convolutional Encoder-Decoder
Pooling Indices
Conv + Batch Normalisation + ReLU
Pooling
Upsampling
Softmax

Figure 6: Sketch of the architecture of SegNet: the encoder, the decoder and the final classification layer, as well as the skip connections between encoder and decoder.

Segnet consists of three components: encoder, decoder and a final classification layer. The encoder is composed by the 13 convolution layers of VGG-16, from which the final fully connected layers have been subtracted reducing then the number of parameters. Each encoder layer has a relative decoder layer and hence 13 decoding layers are had, followed by a multi-class softmax classifier. A representation of the SegNet structure can be observed at Figure 6.

The *encoder* part is composed as a stack of the following structure: convolution layer with ReLU activation, batch normalization and max-pooling layer of window 2x2 with stride 2. This last layer helps the net to be more robust against shits and space variations, however several layers of pooling can induce loss of spatial resolution. Hence, to avoid this loss the indexes of the max-pooling layers are stored to be used once again at the decoder part.

Then the *decoder* part upsamples the received feature maps using the stored pooling indexes as depicted in 7, thus avoiding any learning parameter in the upsampling step. As the resulting output is notably sparse, a convolution layer and batch normalization layers are applied to obtain better resolution and denser outputs. Has to be noted that only storing the pooling indexes is computationally more efficient than storing all encoder feature maps, and regarding pragmatic use, there is only a little loss on resolution.

And finally the classification layer with a softmax classifier giving K channel image of probabilities (one for each class). The class selected is the one with maximum probability.

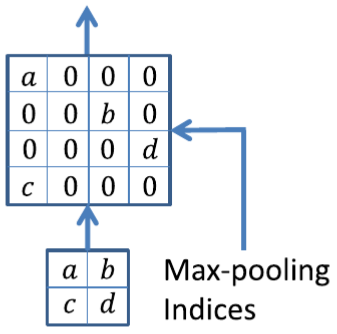

Figure 7: Illustration of the use of the saved max-pooling indexes during the upsampling procedure.

Among the variants appearing in the original paper, SegNet basic has been chosen for study. It consist of a smaller version of Segnet which only has four encoders and four decoders. The main differences, apart from size, are that no bias and ReLu units are used in the decoder part and that a constant kernel size of 7 x 7 is used in all encoder and decoder layers.

3.3.3 Results

The code used for this section can be found at tkuanlun350/Tensorflow-Segnet.

Code adaptation. Several changes were made to the code in order to be able to apply it to our dataset and environment:

- Image size defintion
- Number of classes
- Form of access to dataset
- Program parameters for ablation purposes.
- Add metrics: F1, precision, recall, accuracy and accuracy per class.
- Possibility of doubling the filters at each convolution layer.
- Added data augmentation methods: mirroring and scaling.

After several finetunning purposed runs of the program the hyperparameters of the network has been set to the following values:

- Batch size 32 (16 if memory problems)
- Learning rate 0.01

As optimizer Adam is used.

Ablation Results. To see which of the different possible configurations was the best performing one several runs have been carried out regarding number of filters, data augmentation and class balancing. The number of steps for training have been defined as 40000.

As first results obtained, the performance in the validation set for the original structure and for the structure with doubled filters. Results can be found in table 4. As can be seen the doubled filters structure obtains a better result regarding all the performance metrics than the original structure. Hence, and following the procedure established in methodology, this modification is set as the momentarily best structure and the following ablations will be added to it.

Architecture	**mIoU** (%)	**Accuracy** (%)	**F1** (%)
Normal	38.80	94.87	54.34
Doubled filters	39.17	94.79	54.49
Doubled Filters + Data Aug.	23.28	89.24	33.21

Table 4: Performance results on validation dataset for the original structure and the architecture with doubled filters. Also performance metrics included for the best of the two previous modifications plus data augmentation.

Regarding the case of data augmentation the results can also be observed at table 4. In this case, as with ICNet, the results has not improved with the two methods of data augmentation but the contrary, it has got poorer. In any of the performance metrics the result is better for the case with data augmentation. In Figure
refsegnet:filters the representation of training for both the doubled filter structure and the same but with data augmentation can be observed. As seen in the images, in the data augmentation case there is less distance between the performance in the training set and in the validation set than in the case without data augmentation. Nevertheless, the performance is worse in the data augmentation case where it does not grow at the same pace than in the case without it.

Next results, as shown in table 5, are in regard the weighting scheme strategy. In this case, the direct strategy has been ruled out due to its results with the ICNet network. Hence, only has been taken into account the outer strategy. In the table the performance regarding global mIoU and Accuracy per class is considered among the doubled filters structure and its weight balancing variants. As seen, the best performing one, regarding mIoU, turns out to be the doubled filter structure without any balancing scheme. Nevertheless, if mean accuracy per classs is taken into account, the best performing network is the doubled filter structure plus outer weighting scheme with exponential weighting.

Final Results.

As the best model regarding mIoU has been the one with the filters doubled, a run of 90k steps has been carried out. The results on the test set can be seen at table 6. As seen the performance on test results has dropped a bit compared to validation results on table 4. Also to remark the fact that the performance regarding the mteric F1 is also quite low.

In figure 9 examples of the inference produced by the doubled filters Segnet structure can be observed. Note the lack of definition in most of the cases and how several parts are

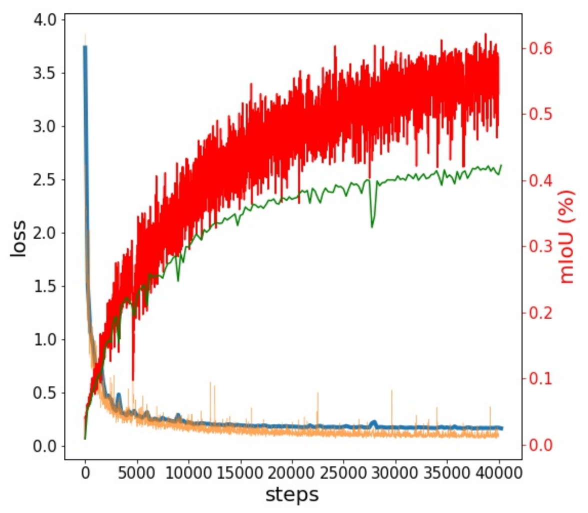

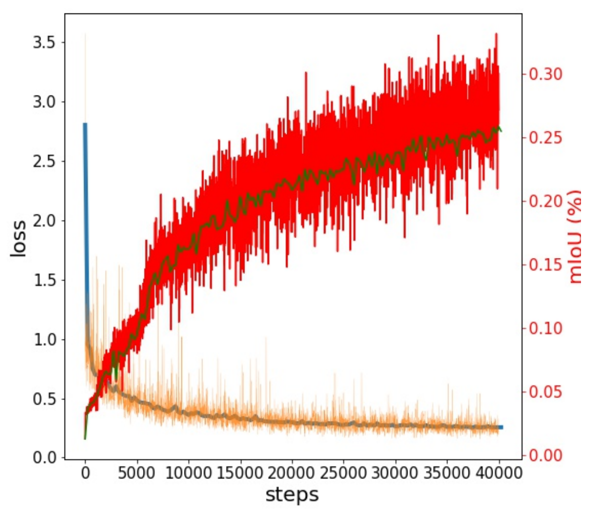

Figure 8: Loss plots for both doubled filters (left) and doubled filters with data augmentation (right) Segnet architectures. (Blue) Validation loss, (Orange) Training Loss, training mIoU (red solid line) and validation mIoU (green line).

	mIoU (%)	Accuracy per Class(%)													
Architecture	**All Classes**	**All classes**	**Background**	**Head**	**Torso**	**U.Legs**	**L.Legs**	**Neck**	**Shoulder**	**U.Arms**	**L.Arms**	**Feets**	**Hands**	**Fingers**	**Toes**
Double Filters	[39.17]	49.9	99.1	84.2	70.9	63.2	58.4	58.1	51.8	52.7	43.9	39.9	28.8	12.4	9.8
DF + W1 (Outer)	38.8	55.6	97.5	90.3	74.2	66.8	61.8	58.3	65.1	62.0	49.6	42.0	36.3	25.3	14.2
DF + W2 (Outer)	21.65	[56.3]	78.18	79.8	65.6	60.0	57.1	85.8	71.1	52.5	51.8	44.2	41.7	34.1	38.4

Table 5: Performance results on validation dataset for the doubled filter structure and the same architecture but with loss weighting for each setup. Here W1 indicates the inverse frequency weithing and W2 the exponential weighting (DF, i.e. doubled filters). Between brackets the best perfoming scheme in both mIoU and mean Accuracy per class.

Architecture	**mIoU** (%)	**Accuracy** (%)	**F1** (%)
Normal	33.59	94.62	44.32

Table 6: Performance results on test set for the doubled filters structure with a training of 90k.

confused (for example, toes; in general those who have a left-right version).

3.3.4 Analysis and Conclusions

Regarding results shown in table 4, it can be seen that the doubled filter structure has a better performance in the validation set. This can indicate that, denoted the variability in the data and the complexity of the original structure, an augmentation of the complexity of the structure, in our case by doubling the convolution filters, improves its result because it is able to capture more patterns and structures in the data. If the complexity of the original structure were enough the effect of doubling the filters would be a loss in the performance in the validation dataset. In our case, due to the size of SegNet (only 8 layers in total), it was logical that it would be benefited from the increase in complexity.

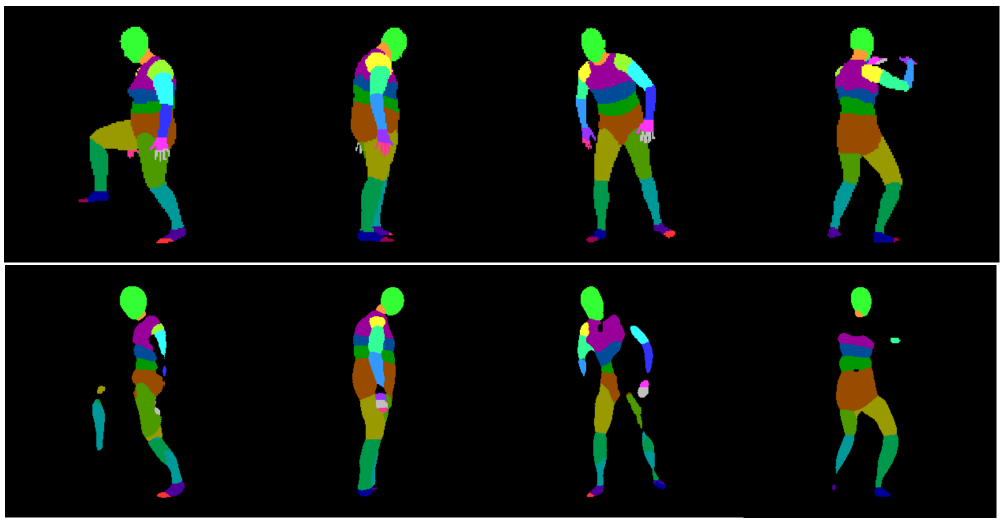

Figure 9: First row: ground truth examples. Second row: inference results with best Segnet model.

Then, also looking at table 4, it can be observed that the data augmentation addition has been of no profit for the performance of the structure. It could be that the data augmentation methods, mirroring and scaling, were not the best ones for this dataset. Adding other data augmentation procedures, such as noise addition, would help to clarify this idea. Nevertheless, although the performance is worse in the data augmentation case, it can be observed a phenomena that would be expected in a training to which data augmentation has been added. That is, the distance between the performance in the training set and in the validation set is less than in the case without data augmentation. This is due to the fact that while training the net gets more robust to variations in the inputs and hence is more prepared against unseen data, thus not downgrading so much its performance in the validation dataset. This phenomena can be observed at Figure 8.

Regarding the weighting scheme procedure (results shown in table 5), the best performing structure, regarding mIou, is the one with no weighting scheme. However, regarding mean Accuracy per class, the best performing one is the doubled filter structure but with outer balancing and exponential weighting. This difference in the best performing network regarding the metric used has an explanation. As mIoU considers areas and its extension it is highly influenced by the classes that occupy a large portion of the image. Hence, when classes are balanced the loss of definition in the high portion classes in favor of minority classes makes the mIoU performance drop down. Meanwhile, the accuracy as is a relative value that only considers the pixels inside the class it is not affected by the portion of the area to respect the whole image. This is the reason why the class balancing scheme helps to improve the mean accuracy per class but drops down the mIoU. Nevertheless, as our main metric is mIoU, our best structure is the doubled filters with no weighting scheme.

In the case of the final results a great drop in the performance regarding mIoU has been observed in the test set compared with the validation results. It could be thought that overfitting during training was the cause of this, but the training and validation loss plot, as seen in Figure 10 does not indicates clearly a case of overfitting. The results regarding mIoU are way down the published results on the SUN RGB-D dataset [*] for the Segnet basic variant which is the one that we use. The published results withstand a value of 46.3 % mIoU. It also surprises the result regarding F1 metric which is quite low. This poor results

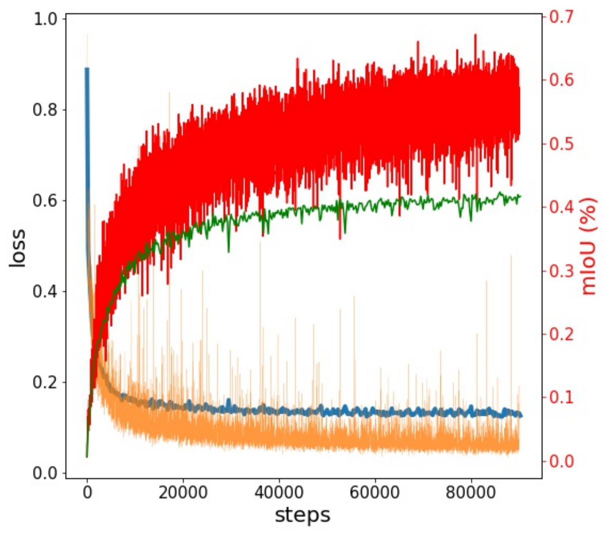

Figure 10: Plot of the training for the doubled filters structure (90k steps). The values shown are training mIoU (red), validation mIoU (green), training loss (orange) and validation loss (blue). As seen no overfitting is apparent.

can be observed in the qualitative results in Figure 9, which show the lack of definition and lack of some body parts, as well as the confusion between some parts (those which have right-left counterparts).

As a conclusion, in the Segnet basic case, the doubled filter structure have proved to be better than the original one, meaning that there was room for more complexity in the model given the variability/diversity of the data. Both data augmentation and balancing scheme has proven to be not useful in terms of mIoU. The final results, both qualitative and quantitative, out stand due to its low performance and quality.

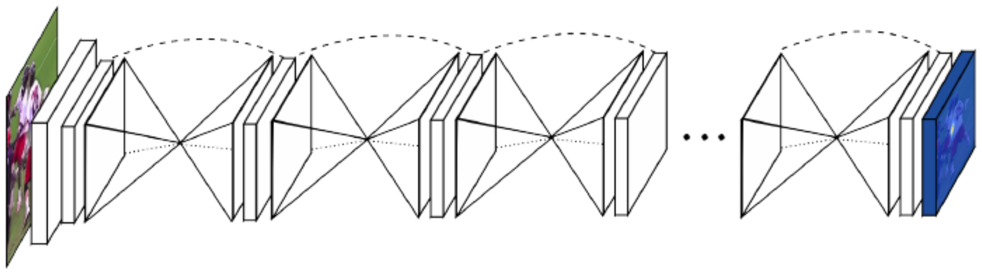

Figure 11: Simple representation of stacked hourglass network.

4 Specialized Networks

4.1 Stacked Hourglass

4.1.1 Introduction

Determining an accurate representation of the pose of a human body through its joints locations is useful for high level tasks such as action recognition. Early works devoted to pose determination used hand-crafted image features and elaborated structure prediction methods. However, with the advent of convolutional networks, the traditional pipeline was superseded and substituted by this new structure which provided significant improvements on the previously obtained results.

Following these new advances, the stacked hourglass model was developed specifically thought to the task of human pose estimation. As many convolutional procedures which produce pixel-wise outputs, the hourglass module captures features across different scales by the use of pooling and subsequent upsampling. Then multiple hourglass modules are stacked consecutively creating the final stacked hourglass network. This repetition allows for repeated top-down and bottom-up inference across different scales which, altogether with the intermediate supervision at the end of each module, enable a substantial improvement of performance.

In our case, and although the network was thought for pose estimation, the input and output of the network have been changed. This change obeys the need stemming from our semantic segmentation task. Nevertheless, with the exception of the input, output and loss function, the structure of the network has been kept the same proving its efficiency and versatility. Altogether with these changes, the two experiments described in 4, have been carried out to try to state ways by which better results could be obtained either transforming the supervision pipeline or expanding the stacked hourglass network.

4.1.2 Description

The stacked hourglass network as its own name indicates is composed by several hourglass modules added in a consecutive manner. An overall example of the structure can be observed at Figure 11. Each of the hourglass modules allow for bottom-up, top-down inference.

A hourglass module, as depicted in Figure 12, is set up in the following way: convolutional and max pooling layers are used to capture features down to a certain resolution.

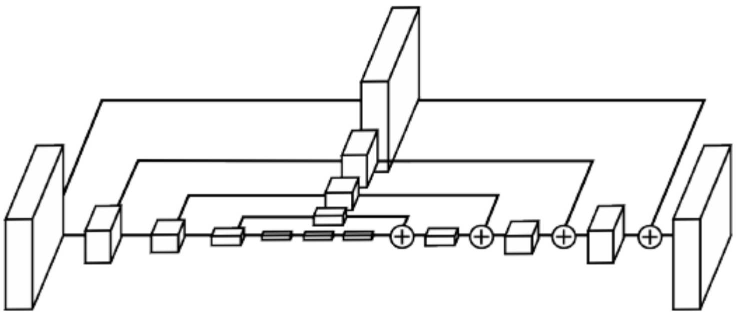

Figure 12: Representation of an hourglass module where each of the boxes represent a residual module.

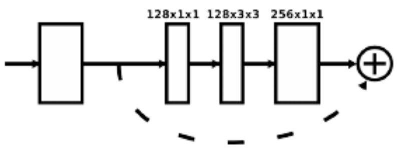

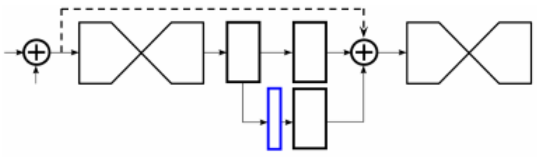

Figure 13: Left: residual module used all through the network. **Right**: illustration of the intermediate supervision process. The networks branches and a loss is applied to a semantic segmentation output. Then, this output, after having applied convolutions to match the number of channels is added to the main data pipeline.

Before each pooling, the network branches off an applies more convolutions to this branching. Once arrived at the lowest resolution, the upsampling process begins, in which nearest neighbor upsampling is used. During this process feature maps coming from the down sampling part and this up sampling part are merged by element wise addition. After reaching the input resolution two rounds of convolutions are applied to the output to obtain the final network prediction. In the original case probability heatmaps of the joint locations were generated, in our case, semantic segmentation of each of the body parts is produced as final output.

Due to performance improvements the convolution layers do not hold big filters: specifically, there are no filters bigger than 3x3. Also, reduction steps of convolution with filters 1x1 after each module, as well as residual modules, are implemented for the same reasons. A representation of a residual module can be observed at Figure 13.

It must be noted that, in the original network, the input was 256x256 while in our case is 320x320. Also, in the original network, the dimensions were reduced to 64 by a round of convolution with kernels 7x7 and stride 2, a residual module and a max pooling layer. In our case the max pooling layer has been deleted and the stride has been reduced to 1 in order to operate at the input resolution.

The fact of stacking several modules, where the input of the following is the output of the previous, provides a mechanism of repeated bottom-up, top-down inference, producing a continuous refinement of the estimates and features all over the image. The key to this point is the use of intermediate predictions at each module to which a loss applied. As a high level understanding of features is required to produce predictions the intermediate supervision is executed at the end of the upsampling process. This predictions came from a branch of the original pipeline and are reintroduced in the stream trough a 1x1 convolution

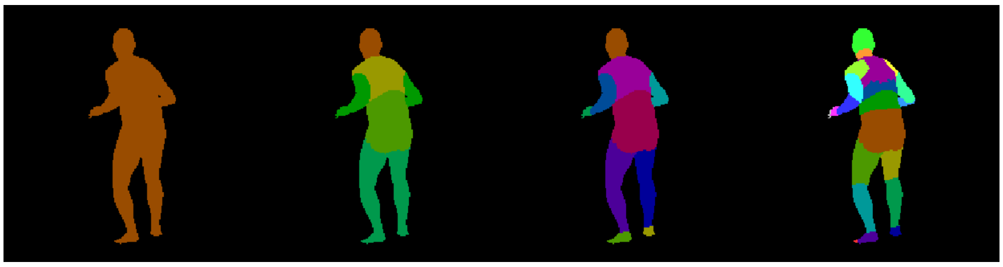
Figure 14: Different ground truth resolutions, one for each module. The idea is to learn a progressive refinement of the real ground truth.

to recover the required number of channels. This final output is served as input for the next module. A representation of these intermediate outputs can be found at Figure 13. Nevertheless, it must be noted that the las output of the network is the one used as final prediction, the intermediates are only used for training the network through a loss.

4.1.3 Experimental Procedure

In this section, a specialized networks will be tested with the SURREAL dataset: Stacked Hourglass. As the network was originally devoted to pose estimation some parts of the code has been changed. The most important ones are: data input and output streams and data reading, the loss and performance metrics. Regarding the loss it has been changed from *sigmoid crossentropy loss with logits* to *sparse softmax crossentropy with logits*, just to adapt it to the nature of the data. The metric was originally a measure of the distance error between the predicted body joint and the real one. This has been changed to the previously used metrics: mIoU, F1, accuracy and accuracy per class.

Also,regarding the last section of general networks, the experimental procedure is changed. Instead of applying variations such as data augmentation or loss weighting, the data structure and the network will be modified directly.Firstly, the plain network will be trained and tested with no modifications to see which are the baseline results to which compare with. Next, two experiments will be carried out to see if the performance results can be improved.

The first experiment consists in arranging the ground truth labels. In the stacked hourglass there are several concatenated modules where the a loss between output of the module and the ground truth is generated. This allows for a refinement of the predictions. Hence, the experiment consists in having a different ground truth in each module. In the first module the ground truth would only regard the body and the background. In the following modules the body will be further partitioned in different body parts in a consecutive manner. For example, in the second module, the ground truth could regard, as differentiated body parts, the head the torso, arms and legs. In the next module, the arms will be split in two corresponding parts: upper and lower arm. This is done consecutively at each module until arriving at the last one where the complete ground truth is used. An example of this procedure for a stack of 4 modules can be seen at Figure 14. The purpose of this strategy is to make the network learn the data structure in a consecutive and refined way: first, will learn to differentiate the body from the background, next arms, legs and torso inside the body, and so on until the complete ground truth.

The next experiment consists in the following: include another module (or modules) in

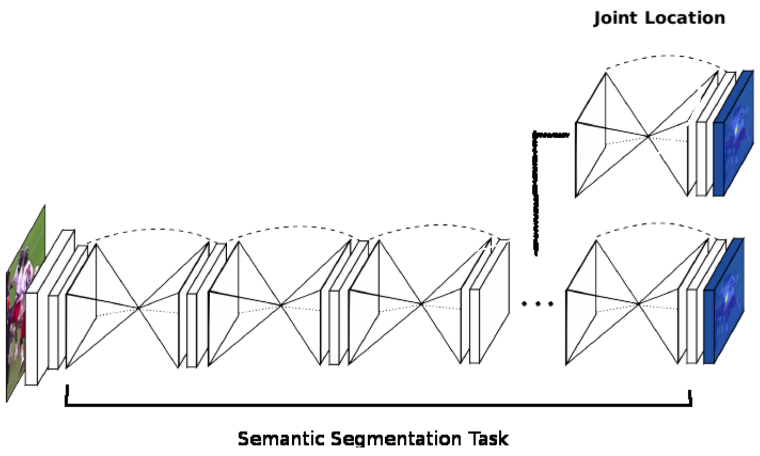

Figure 15: Representation of the multitask stacked hourglass. In this case with only one module devoted to the auxiliary task. The whole main network is devoted to semantic segmentation while the parallel module is devoted to joint location.

parallel devoted to another task. As the original network was devoted to pose estimation (body joint location) the auxiliary task has been defined to be this original purpose. As seen in 15 the experiment consists in deviate the output of certain chosen module an introduce it both in the ordinary next module and into another parallel module. This new branch will be dedicated to joint location so ground truths must be generated or chosen. In this case, the SURREAL dataset provide (x,y) coordinates. Nevertheless, another option, if these information is not had is to consider the central point location of each of the body parts. Both joint types are shown in 16.

The purpose of this experiment is to see if adding this branch devoted to another task can help improve the results on the segmentation task. The junction between of both types of data is obvious since the joints indicate a delineation of the figure and also its position. However, the intention is not to obtain results on joint location but to see if this improves semantic segmentation.

4.1.4 Results

In this section performance results will be shown regarding the plain hourglass, the different resolutions experiment and the experiment of adding a joint detection branch.

4.1.5 Analysis and conclusions

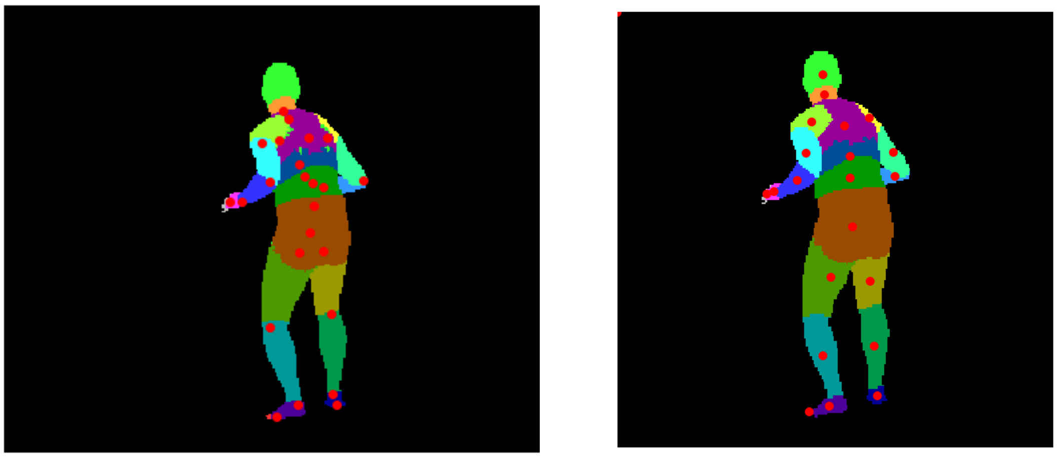

Figure 16: Location of the different joints. **Left**: joints provided by the SURREAL dataset. **Right**: central part point location.

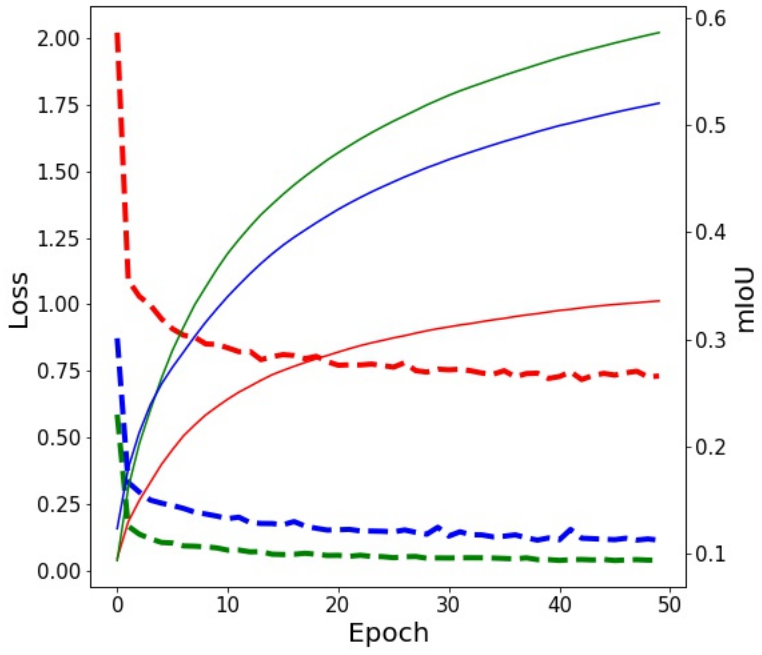

Figure 17: Plot of the loss and mIoU performance on the validation set while training. Dashed lines represent loss while solid lines represent mIoU values. Red lines correspond to the different resolutions scheme, blue lines to the scheme with the joint location branch and green lines to the original net.

5 Network Comparison